Electronic Supplementary Material (ESI) for Chemical Science.
This journal is © The Royal Society of Chemistry 2018

Supplementary Information

An "All-in-One" Antitumor and Anti-Recurrence/Metastasis Nanomedicine with Multi-Drug Co-Loading and Burst Drug Release for Multi-Modality Therapy

Ji-Chun Yang [1], Yue Shang [2], Yu-Hao Li [2], Yu Cui [1], Xue-Bo Yin[1,3,]*

[1] State Key Laboratory of Medicinal Chemical Biology and Tianjin Key Laboratory of Biosensing and Molecular Recognition, College of Chemistry, Nankai University, Tianjin, 300071, China

[2] Tianjin Key Laboratory of Tumor Microenviroment and Neurovascular Regulation, School of Medicine, Nankai University, Tianjin, 300071, China.

[3] *Collaborative Innovation Center of Chemical Science and Engineering (Tianjin), Nankai University, Tianjin, 300071, China*

EXPERIMENTAL SECTION

Materials and reagents. Copper chloride ($CuCl_2$), trisodium citrate dehydrate ($Na_3C_6H_5O_7 \cdot 2H_2O$), sodium sulfide nonahydrate ($Na_2S \cdot 9H_2O$), zinc nitrate hexahydrate [$Zn(NO_3)_2$], 2-methyl imidazole (HMeIM), and potassium permanganate were purchased from Fuchen Chemical Reagent Co., Ltd., Tianjin, China. Dopamine hydrochloride, doxorubicin hydrochloride (DOX) and protoporphyrin IX (PpIX) were bought from Sigma-Aldrich Co., Ltd., Shanghai, China. CpG (1826) oligodeoxynucleotides (5'-TCCATGACGTTCCTGACGTT-3') were synthesized by Sangon Biotechnology Co., Ltd., Shanghai, China. All of the other reagents were supplied by Shanghai Aladdin Chemistry Co., Ltd without further purification. Ultrapure water was used throughout all experiments and to prepare all solutions.

Instrument and characterization. The morphologies of samples were observed using a transmission electron microscopy operated at an accelerating voltage of 200 kV (TEM, JEM-2010HR, Japan). Thermogravimetric analysis (TGA) measurements were performed on a PTC-10ATG-DTA equipment heated from room temperature to 700 °C at a ramp rate of 10 °C min^{-1} under air. X-ray diffraction (XRD) patterns were conducted with a D/max-2500 diffractometer (Rigaku, Japan) using Cu-Kα radiation (λ=1.5418 Å). N_2 adsorption-desorption isotherms were recored by a NOVA 2000e surface area and pore size analyzer (Quantachrome, Florida, FL, USA) at 77 K. X-ray photoelectron spectrum (XPS) was recorded using an Axis Ultra DLD with nonmonochromatized Al Kα radiation. A Zetasizer Nano-ZS (Malvern, England) was selected to measure the hydrodynamic sizes (DLS) and zeta potentials. UV-visible

absorption spectra were recorded by a UV-2450-visible spectrophotometer (Shimadzu, Japan). Inductively Coupled Plasma-Atomic Emission Spectrometer (ICP-AES, Thermo, USA) was used to validate the content of CuS, ZIF-8, PDA and MnO_2 in the products. The transverse relaxivity times and T_1-weighted MR images were conducted using a MRI system (1.2 T, Huantong, Shanghai, China). Thermal IR images *in vitro* and *in vivo* were acquired by Ti25 IR thermal camera, Fluke, USA.

Preparation of CuS nanoparticles (NPs). CuS NPs were prepared via a reported method with slight modification.[1] Typically, 68.2 mg $CuCl_2$ and 80 mg $Na_3C_6H_5O_7 \cdot 2H_2O$ were dissolved in 90 mL ultrapure water under magnetic stirring, then 10 mL $Na_2S \cdot 9H_2O$ solution (9.6 mg mL^{-1}) was added dropwise. After processing at 90 °C for 15 min, the solution color turned to dark green, indicating the successful formation of CuS NPs. Finally, the obtained citrate-coated CuS NPs were stored at 4 °C for later use.

Preparation of CuS@ZIF-8 nanocomposites (NCs). To synthesize CuS@ZIF-8 NCs (denote as CuZ, and the abbreviations of all the products were listed in Table S1), 230 mg HMeIM was dissolved in 5 mL CuS solution firstly. Then, 1 mL $Zn(NO_3)_2$ methanol solution (12.42 mg mL^{-1}) was added under gentle stirring. The mixture left undisturbed at room temperature for 30 min. After the reaction, the resulting NCs were centrifuged at 12000 rpm for 5 min and washed with methanol to obtain CuS@ZIF-8 NCs for further use.

Preparation of CuS@ZIF-8@PDA (CuZP) NCs. The above CuZ NCs were re-dispersed in 1.5 mL methanol and 3 mL Tris-HCl mixture buffer solution (pH 8.5),

followed by adding 6 mg dopamine hydrochloride. This organic-inorganic hybrid buffer system slowed down the self-polymerization reaction of dopamine and made PDA layer coated on the surface of ZIF-8 uniformly.[2] Then, the suspension was stirred under air condition for 4 h, and CuZP NCs was collected and washed with methanol for three times to remove the unpolymerized dopamine.

Preparation of CuS@ZIF-8@PDA@MnO_2 (CuZPMn) NCs. In a typical preparation of CuZPMn NCs, 5 mL $KMnO_4$ solution (0.2 mg mL^{-1}) was added to dropwise 2 mL of 1 mg mL^{-1} CuZP NCs suspension, and then the mixture was stirred for 5 min at room temperature. The CuZPMn NCs were obtained by centrifugation and suspended in ultrapure water at 4 °C.

Drug loading and release profiles from CuZPMn NCs. The one-pot drug loading method was applied to encapsulate PpIX and DOX together during the preparation of ZIF-8. 1.5 mg PpIX and 4 mg DOX was introduced into $Zn(NO_3)_2$ methanol solution. CuS NPs HMeIM were prepared in their aqueous solution. The methanol solution was mixed with the aqueous solution for the formation of PpIX-DOX-CuS co-loaded ZIF-8 NCs. Then the products were washed three times with methanol. 80 μg 1 mL mono-dispersed the multi-drug loading NCs were supplemented with 2 μM CpG to wrap CpG. The mixture was vigorous stirred for 2 hours and centrifuged to remove unbound CpG. The residual PpIX, DOX, and CpG ODNs in the supernatants were determined by UV-Vis measurements, to calculate the loading e□ciency (LE) with Equation (1):

$$LE\ (\%) = \frac{weight\ of\ loaded\ PpIX\ or\ DOX}{original\ weight\ of\ PpIX\ or\ DOX} \times 100\% \qquad (1)$$

Single-DOX was taken as an example to investigate the drug release properties of CuZPMn NCs to avoid the mutual interference between different drugs. The cumulative drug release experiment was carried out with a dialysis bag diffusion technique at 37 °C. 5 mg DOX-loaded NCs was dispersed in 3 mL of PBS solutions (pH 7.4 or pH 5.0) and sealed in a dialysis bag (MWCO 4000 Da). The dialysis bag was submerged in 30 mL of PBS solutions and stirred for 12 h. At predetermined time intervals, 100 μL PBS solution was collected to detect the content of DOX. In the group of NIR irradiation, the CuZPMn@DOX NCs were exposed to an 808 nm NIR laser (2 W cm^{-2}) for 5 min before the media was tested to determine the release amount by using UV-Vis spectra, and the release efficiency (RE) was calculated according to Equation (2):

$$RE\ (\%) = \frac{weight\ of\ released\ drugs}{weight\ of\ loaded\ drugs} \times 100\% \qquad (2)$$

***In vitro* singlet oxygen generation.** The singlet oxygen ($^1O_2$) generation capacity was tested with 9, 10-anthracenediyl-bi(methylene) dimalonic acid (ABDA) assay. The solution containing 50 μg mL^{-1} CuZPMn@PpIX NCs and 100 μM ABDA was irradiated for 60 min under 655 nm laser with the power intensity of 0.3 W cm^{-2}. At each predetermined time interval, the UV absorbance spectra of the solution was recorded. The stability of ABDA to 655nm laser irradiation at the same condition was also tested as control.

The generation of reactive oxygen species (ROS) from CuZPMn, CuZP@PpIX and CuZPMn@PpIX with or without 655 nm laser irradiation were also detected using a single oxygen probe DCFH-DA. 4T1 cells were seeded in a 24-well plate at a density

of 5 × 10^3 cells per well and incubated with 200 μg mL^{-1} CuZPMn, CuZP@PpIX and CuZPMn@PpIX overnight. After that, the cells were washed with PBS for three times and replaced with fresh medium. 50 μL of DCFH-DA (100 μM in DMSO) was added to the cells and incubated for another 0.5 h at 37 °C. The cells were irradiated with or without 655 nm laser (0.3 W cm^{-2}) for 10 min. Then the generated ROS were monitored by confocal laser scanning microscopy with an excitation of 488 nm and emission of 530 nm. The generation of ROS in 4T1 cells without adding NCs under 655 nm laser irradiation for 10 min or not were taken as control.

***In vitro* and *in vivo* photothermal performance.** *In vitro* photothermal performance of CuZPMn NCs was investigated by measuring the temperature changes of CuZPMn NCs suspensions with the concentrations ranged from 0 to 200 μg mL^{-1} at 808 nm with output power of 2 W cm^{-2} for 10 min. The changed temperature was recorded and imaged simultaneously with an infrared thermal imaging camera (FLIR-A300, FLIR Systems Inc., U.S.A.).

For *in vivo* photothermal effect evaluation, 4T1 tumor-bearing Balb/c mice were administrated with 200 μL of 1.5 mg mL^{-1} CuZPMn NCs suspension and irradiated with 808 nm NIR laser at the power density of 2 W cm^{-2} for 10 min at 10 h post intravenous injection. The tumor temperatures of mice were also recorded with the IR camera thermographic system. The tumor-bearing mice injected with PBS were selected as the control.

Cell culture. Both RAW264.7 cells (murine macrophage-like cell) and 4T1 (breast cancer cells) were grown in DMEM medium supplemented with 10% fetal bovine

serum (FBS) and 1% penicillin-streptomycin at 37 °C in a humidified atmosphere with 5% CO_2. The medium was replaced every three days, and the cells were digested by trypsin and redispersed in a fresh culture medium before plating.

Cellular uptake and cytokine assays. To quantify the cellular uptake efficiencies of the NCs, RAW264.6 and 4T1 cells were seeded in a 6-well plate at a density of 2×10^7 per well and incubated with 200 μg mL^{-1} CuZPMn overnight. Then the cells were collected and washed three times with PBS. RAW264.6 and 4T1 cells were re-suspended into 500 μL PBS and digested with nitric acid for inductively coupled mass spectrometry (ICP-MS) of Mn.

Furthermore, the cellular uptake efficiencies of the NCs were also investigated by confocal fluorescence images of RAW264.7 cells. RAW264.7 cells were plated in a 24-well plate (1×10^6 cells per well) and incubated overnight. Then, the cells were incubated with Cy 5 labeled free CpG ODNs alone and CuZPMn@Cy5-CpG NCs with 5 min 808 nm NIR irradiation or without NIR irradiation at 37 °C for 4 h. After the cells were washed three times with PBS to remove the excess materials followed by DAPI staining, confocal imaging of the cells was recorded with an Olympus FV1000 laser scanning microscope equipped with a CCD camera to evaluate the CpG ODNs uptake.

For cytokine assays study, RAW264.7 cells were seeded on 24-well culture plates at a density of 1×10^6 cells per well. After incubation overnight, cells were further incubated with 2 μM free CpG ODNs, 200 μg mL^{-1} CuZPMn, CuZPMn@CpG, CpG encapsulated in CuZPMn during preparation of ZIF-8 and CuZMn@CpG with 808

nm NIR irradiation for 5 min or without NIR irradiation at 37 °C for 8 h. Then the conditioned medium was carefully collected and stored at -80 °C until analysis. The secretion of TNF-α by RAW264.7 cells was determined by enzyme-linked immunosorbent assay (ELISA) using antibody pair specific to these cytokines following the protocol recommended by the manufacturer.

***In vitro* cell viability assay and the synergic therapeutic efficacy.** The *in vitro* cytotoxicity and synergic therapeutic efficacy of the NCs were assessed with standard 3-(4,5-dimethylthialzol-2-yl)-2,5-diphenyltetrazolium bromide (MTT) assay. Briefly, 4T1 cells were seeded in a 96-well plate at a density of 5×10^3 per well and incubated overnight. For PDT and PTT groups, the 4T1 cells were irradiated with 655 nm (0.2 W cm^{-2}) and 808 nm (2 W cm^{-2}) laser for 10 min, respectively. The PDT + PTT group was conducted under 808 nm irradiation for 10 min firstly and then 655 nm for 10 min. Free DOX and chemotherapy + PTT groups were taken as comparison. Immunotherapy group was performed through a 4T1 co-incubated with RAW264.7 cells method. RAW264.7 cells and 4T1 cells were placed in the upper and lower chambers of Transwell plates, respectively. CuZPMn@CpG NCs were added to the upper chamber and incubated with RAW264.7 cells for 8 h, and then the RAW264.7 cells were irradiated by 808 nm laser (2 W cm^{-2}) for 3 min to make CuZPMn@CpG collapse and release CpG ODNs for immune activation. After incubating overnight, the cellular viability of 4T1 cells in the lower chamber was determined by MTT assay.

GSH-responsive T_1-weighted MR imaging and biodistribution and excretion of CuZPMn NCs. MR imaging experiments were performed on a MRI scanner (1.2 T,

Huantong, Shanghai, China). For *in vitro* study, the samples with different Mn^{2+} concentrations range from 0 to 1.0 mM were prepared with CuZPMn NCs under non-reducing (in the absence of GSH) or reducing (in the presence of 4 mM GSH) buffer solutions, respectively. The specific relaxivity values of r1 (mM^{-1} s^{-1}) were calculated as the reciprocal of $1/T_1$ (s^{-1}) at various Mn^{2+} concentrations (mM). For *in vivo* mice MR study, 200 μL of 1.5 mg mL^{-1} CuZPMn NCs suspension was i.v. injected into a 4T1 tumor-bearing mouse for T_1-weighted MR imaging. The images of mice before and after injection at selected time intervals were recorded with a fat-saturated 3D gradient echo imaging sequence (TR/TE = 400/10 ms, 256 × 256 matrices, slices = 3, thickness = 2 mm, averages = 4, FOV = 60×60).

To study the biodistribution of CuZPMn NCs *in vivo*, 200 μL of 1.5 mg mL^{-1} CuZPMn were injected into tumor bearing mice intravenously, and the mice were sacrificed at 4 h, 10 h and 24 h post injection. The tumor and main organs including heart, liver, spleen, lung and kidney were dissected and digested for ICP-MS of Mn to monitor the biodistribution of the NCs. Furthermore, the feces and urine of mice after injection of CuZPMn NCs were also collected to study the excretion of the NCs.

***In vivo* antitumor efficiency evaluation.** Female Balb/c mice (6-8 weeks) used in animal experiments were purchased from the Institute of Hematology & Hospital of Blood Disease, Chinese Academy of Medical Sciences & Peking Union Medical College with the license No. SYXK-2014-0003, Tianjin, China. All animal experimental protocols were approved by the Institutional Animal Care Committee of Nankai University and all methods were carried out in accordance with the relevant

guidelines and regulations from the Institutional Animal Care Committee of Nankai University, China.

The tumors were established by subcutaneous injection of 4T1 tumor cells into the right hind limb of each mouse. When the tumors reached a size of ~100 mm^3, the 4T1 tumor-bearing mice were randomized into eight groups (n = 3 per group) and treated by intravenous injection of PBS, CuZPMn, CuZPMn@PpIX + 655 nm, CuZPMn@DOX (the mass percent of DOX in the nanomedicine was approximate 17%), CuZPMn + 808 nm, CuZPMn@CpG, CuZPMn@PpIX/DOX + 655 nm + 808 nm, CuZPMn@PpIX/DOX/CpG + 655 nm + 808 nm, respectively. The four-modality therapy are not in strict sequence. The PDT therapy was achieved when CuZPMn@PpIX NCs was irradiated under 655 nm laser. The PTT therapy started with the irradiation of 808nm. At the same time, the PTT therapy triggered the release of DOX and CpG for chemotherapy and immunotherapy. All the therapies were repeated every 3 days within 18 days. Tumor sizes and mouse body weights were monitored every 2 days. The tumor volume was calculated according to the equation: volume = (tumor length) × $(\text{tumor width})^2/2$. Meanwhile, main organs of mice were harvested for histological examination.

***In vivo* anti-recurrence and anti-lung metastasis efficacies evaluation.** *In vivo* anti-recurrence and anti-lung metastasis mouse models were established to prove the good efficacy of the immunotherapy. For anti-recurrence efficacy study, 4T1 tumor cells (1×10^7 cells) were suspended in 0.1 mL of PBS and subcutaneously injected into the left hind limb of each mouse of PBS, CuZPMn@PpIX/DOX + 655 nm + 808 nm and

CuZPMn@PpIX/DOX/CpG + 655 nm + 808 nm treated groups on the fifth day after finishing treatments. The volumes of induced recurrence tumors were also recorded every 2 days.

For anti-lung metastasis model, 4T1 tumor cells (1×10^7 cells) were intravenously injected into the mice of PBS, CuZPMn@PpIX/DOX + 655 nm + 808 nm and CuZPMn@PpIX/DOX/CpG + 655 nm + 808 nm treated groups on the fifth day after finishing treatments. On the tenth days after intravenous injection, the lungs of mice were infused with 15% India ink through the trachea, rinsed briefly in distilled water, and soaked in Fekete's solution overnight. White spots on black-stained lungs were marked as tumor metastasis sites. The body weights and H&E staining of lungs were also recorded to monitor the physical conditions of mice.

Statistical analysis. All figures shown in this article were obtained from three independent experiments with similar results. Statistical analysis was performed using Student's *t* test, and results of $p<0.05$ were considered statistically significant.

RESULTS AND DISCUSSIONS

Table S1. Abbreviation names of the nanocarriers in the paper.

Species	abbreviations
CuS nanoparticles	CuS
CuS@ZIF-8	CuZ
CuS@ZIF-8@PDA	CuZP
CuS@ZIF-8@PDA@MnO_2	CuZPMn
CuS@ZIF-8@MnO_2	CuZMn
CuS@ZIF-8/PpIX@PDA@MnO_2	CuZPMn@PpIX
CuS@ZIF-8/DOX@PDA@MnO_2	CuZPMn@DOX
CuS@ZIF-8/CpG@PDA@MnO_2	CuZPMn@CpG
CuS@ZIF-8/PpIX/DOX/CpG@PDA@MnO_2	CuZPMn@PpIX/DOX/CpG

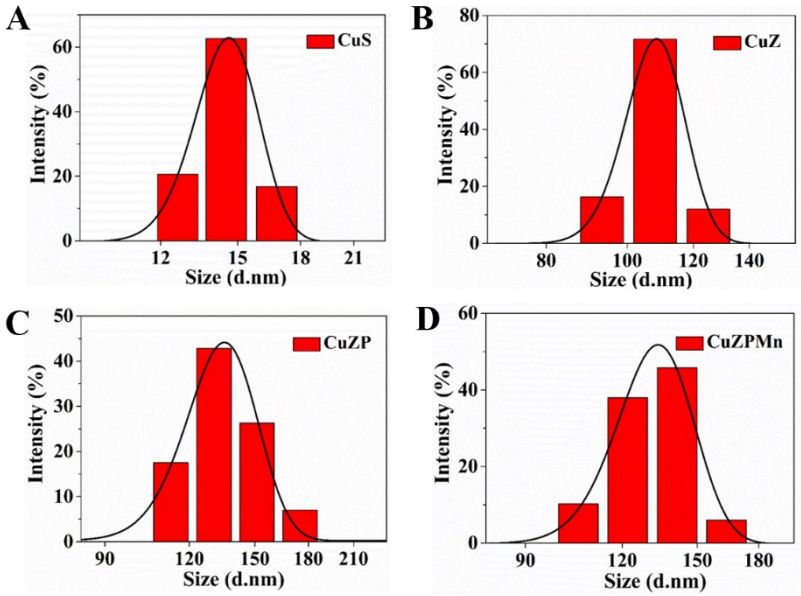

Figure S1. DLS size distributions of all the NCs. (A) CuS, (B) CuZ, (C) CuZP and (D) CuZPMn had relatively narrow size distribution for real application.

Table S2. The content of different ingredients in CuZPMn NCs determined by TGA and ICP-MS. The mass ratios of CuS, ZIF-8, PDA and MnO_2 in CuZPMn NCs calculated from TGA weight loss was consist with that from ICP-AES.

	CuS (%)	ZIF-8 (%)	PDA (%)	MnO_2 (%)
TGA	7.6	37.1	37.0	18.4
ICP-AES	7.1	39.8	32.4	20.7

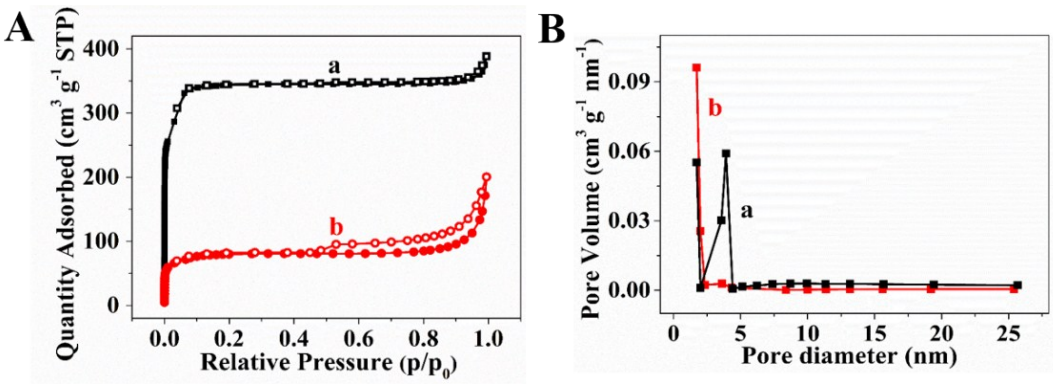

Figure S2. (A) N_2 adsorption-desorption isotherms, and (B) DFT pore size distribution of a) CuZ and b) CuZP. Compared with ZIF-8, the surface area and pore volume of CuZ decreased from 0.49 cm^3 g^{-1} and 1560.0 m^2 g^{-1} to 0.23 cm^3 g^{-1} and 1153.4 m^2 g^{-1} because of the introduction of non-porous CuS NPs in ZIF-8.

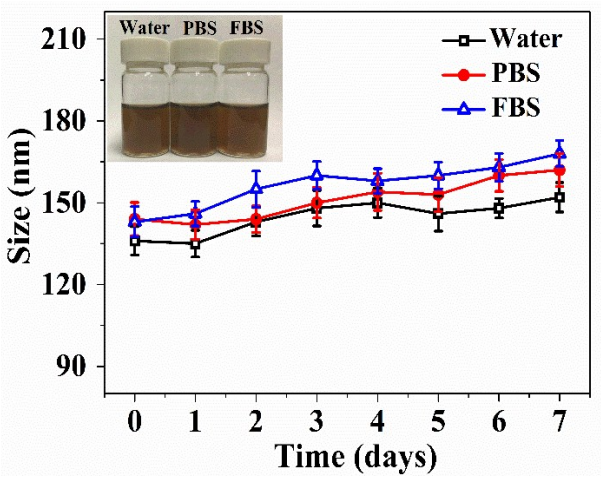

Figure S3. Size distribution of CuZPMn after 7 d of storage. No macroscopic aggregate and precipitate were observed after 7 d of storage in different media at room temperature, which indicating the stability of the NCs.

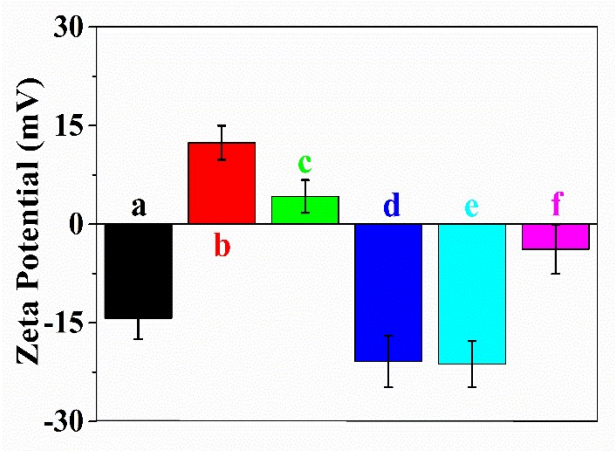

Figure S4. Zeta potentials of different NCs. The different zeta potentials of the products at each step verified the successful attachment of CpG and preparation of the different NCs (a) CuS, (b) CuZ, (c) CuZ@PpIX/DOX, (d) CuZ@PpIX/DOX/CpG, (e) CuZP@PpIX/DOX/CpG, and (f) CuZPMn@PpIX/DOX/CpG.

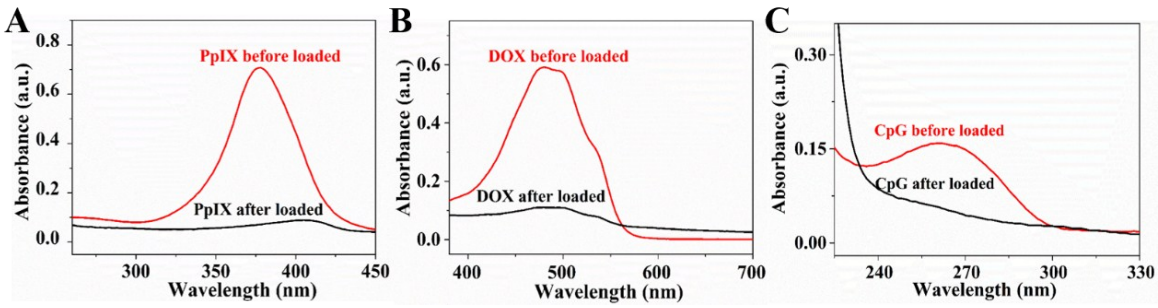

Figure S5. UV-vis absorbance spectra of PpIX, DOX and CpG before and after loading. The loading efficiency was approximately (A) 94% for PpIX, (B) 92% for DOX, and (C) 98% for CpG ODNs.

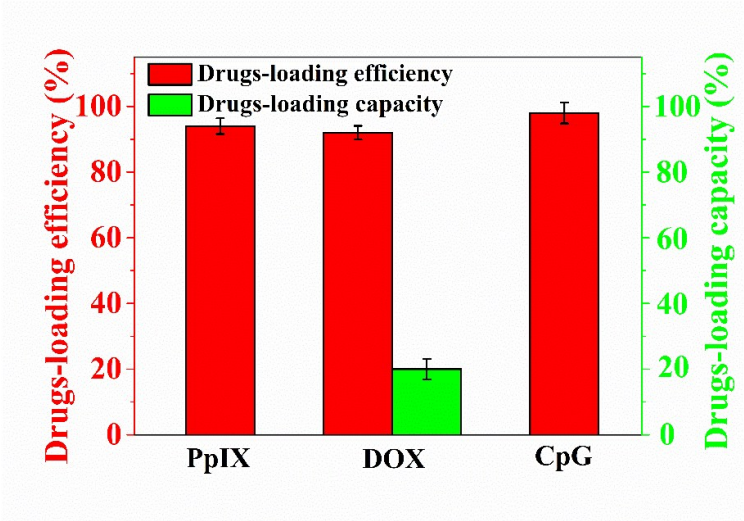

Figure S6. Drugs-loading efficiencies and drugs-loading capacity of CuZPMn NCs.

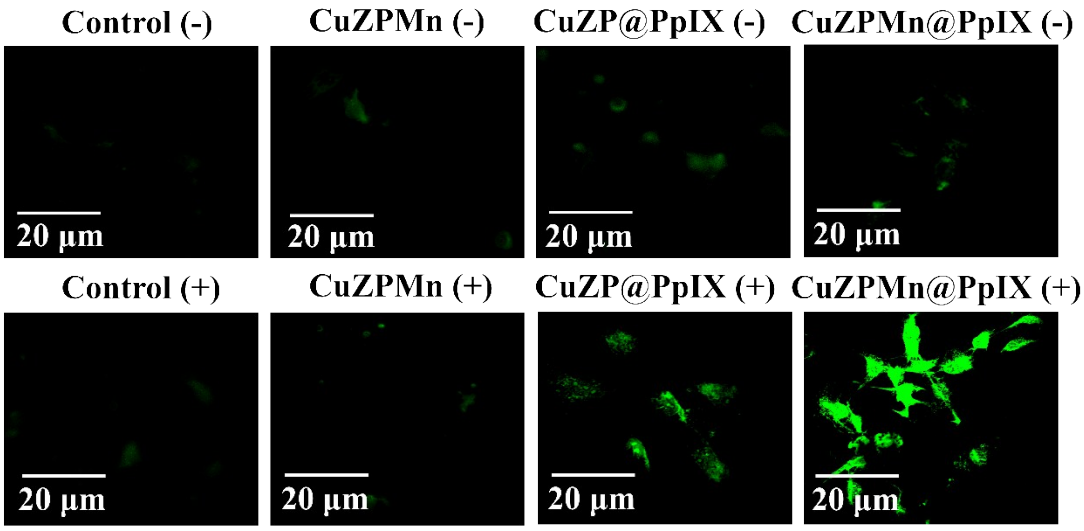

Figure S7. *In vitro* ROS generation of CuZPMn, CuZP@PpIX and CuZPMn@PpIX with or without 655 nm laser irradiation (0.3 W cm^{-2}) for 10 min using DCFH-DA as sensor. "(+)" and "(−)" represent the samples with and without irradiation, respectively.

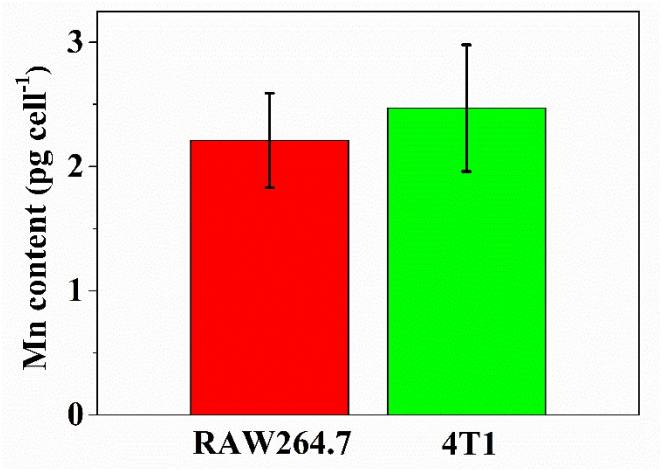

Figure S8. ICP-MS analysis of the cellular uptake of CuZPMn NCs. The intracellular Mn contents in RAW264.7 and 4T1 cells.

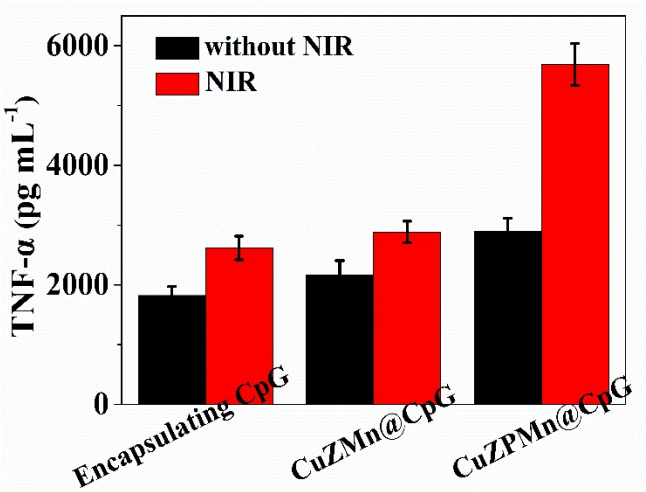

Figure S9. The secretion of TNF-α from RAW264.7 cells stimulated by CpG encapsulated in the internal of ZIF-8 during preparation and without the protection of PDA layer (CuZMn@CpG) groups.

The secretion of TNF-α from internal encapsulating CpG and CuZMn@CpG groups decreased significantly compared with that from CuZPMn@CpG group. It was possibly attributed from the deactivation of CpG induced by methanol and strong oxidizing $KMnO_4$. Thus, CpG wrapped on the surface of ZIF-8, while PDA layer avoided the destruction of CpG and maintained its immune activation ability effectively.

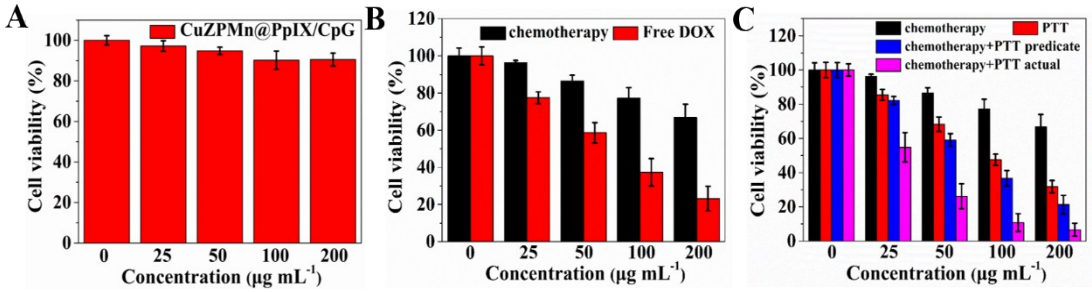

Figure S10. Cell viabilities of 4T1 cells treated with (A) CuZPMn@PpIX/CpG, (B) CuZPMn@DOX without NIR irradiation and free DOX. (C) The predicated and actual effects of cell viability of 4T1 cells treated with chemotherapy + PTT *in vitro*.

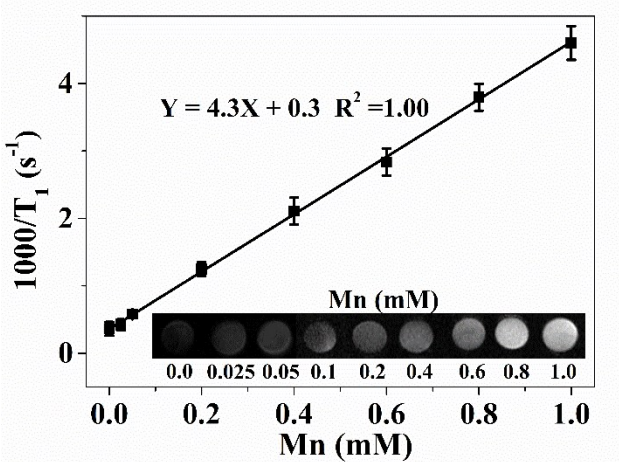

Figure S11. The r_1 relaxivity curves of $MnCl_2$ *in vitro*.

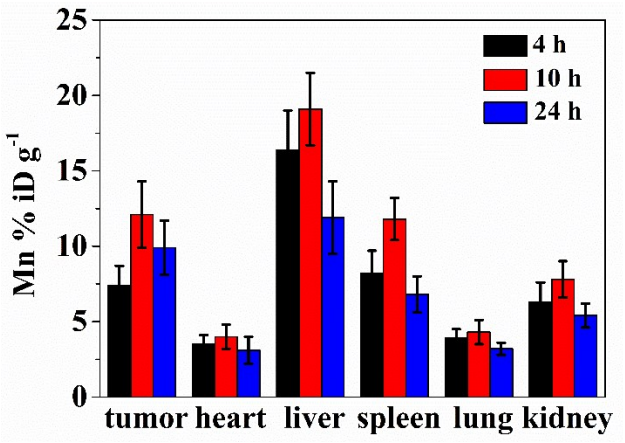

Figure S12. The biodistribution of CuZPMn NCs *in vivo* at 4 h, 10 h and 24 h post injection (% iD means the percentage of the injection dose).

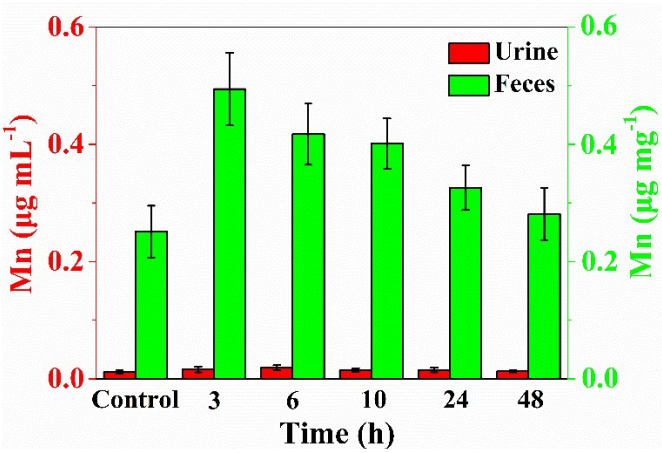

Figure S13. The contents of Mn in urine and feces at different points (3, 6, 10, 24, 48 h) after the injection of CuZPMn NCs.

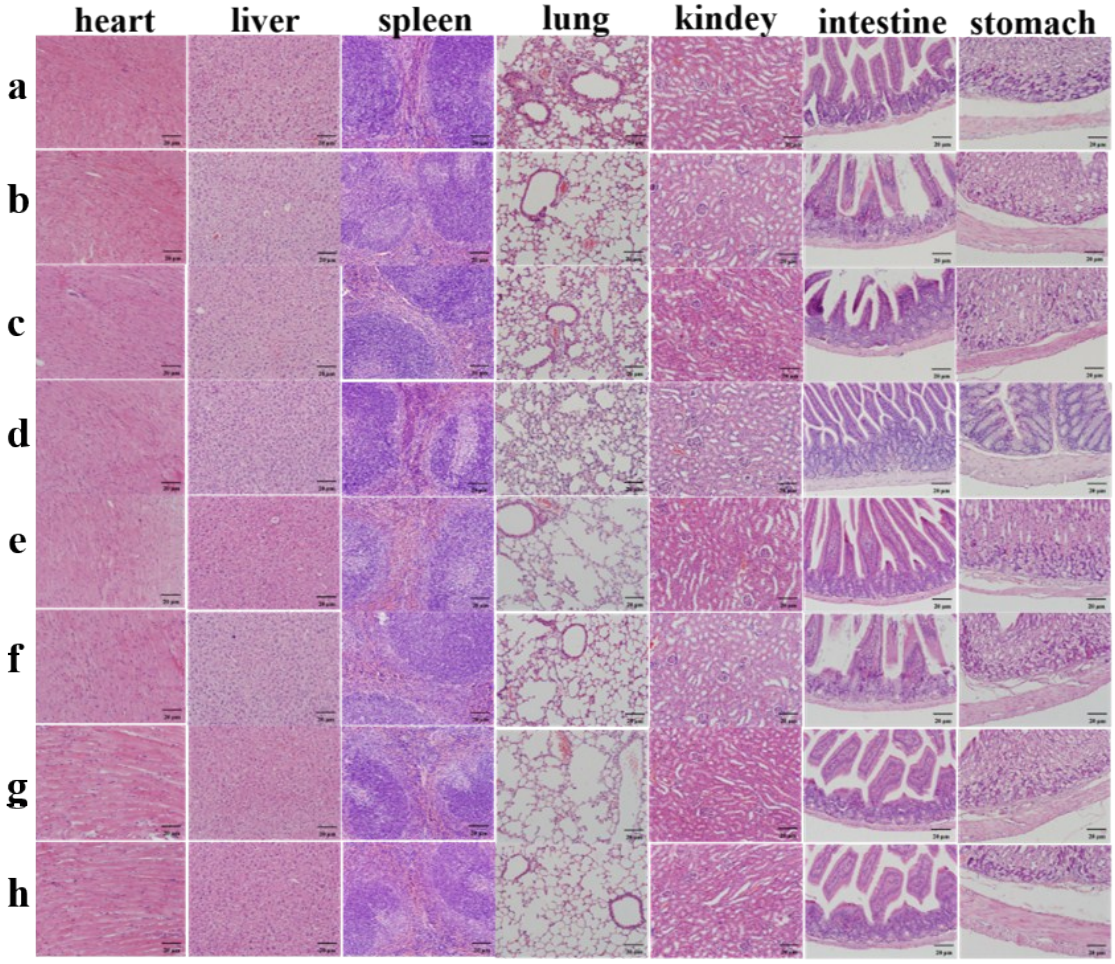

Figure S14. H&E stained images of major organ slices of mice from different groups after 18 days treatment. No pathological changes were noticed for mice after 18 days treatments because of the excellent biocompatibility of the CuZPMn@PpIX/DOX/CpG NCs (a) PBS, (b) CuZPMn, (c) PDT, (d) chemotherapy, (e) PTT, (f) immunotherapy, (g) PDT + chemotherapy + PTT, and (h) PDT + chemotherapy + PTT + immunotherapy.

REFERENCES

1. X. Liu, Q. Ren, F. Fu, R. Zou, Q. Wang, G. Xin, Z. Xiao, X. Huang, Q. Liu and J. Hu, *Dalton T.*, 2015, **44**, 10343-10351.

2. Q. Yue, M. H. Wang, Z. K. Sun, C. Wang, C. Wang, Y. H. Deng and D. Y. Zhao, *J. Mater. Chem. B*, 2013, **1**, 6085-6093.